Korean J. Chem. Eng., **31**(3), 402-411 (2014)
DOI: 10.1007/s11814-013-0215-4

pISSN: 0256-1115
eISSN: 1975-7220

Pressure distribution and wall shear stress in stenosis and abdominal aortic aneurysm by computational fluid dynamics modeling (CFD)

Jong-Beum Choi*, Young-Ran Park, Shang-Jin Kim***, Hyung-Sub Kang***, Byung-Yong Park****, In-Shik Kim****, Yeong-Seok Yang*****, and Gi-Beum Kim*,**,******,†**

*Chonbuk National University Medical Schools, Chonbuk National University, Duckjin-dong 1-Ga, Duckjin-gu, Jeonju 561-756, Korea
**Division of Chemical Engineering, College of Engineering, Chonbuk National University, Duckjin-dong 1-Ga, Duckjin-gu, Jeonju 561-756, Korea
***Department of Pharmacology, College of Veterinary Medicine, Korea Zoonosis Research Institute, Chonbuk National University, Duckjin-dong 1-Ga, Duckjin-gu, Jeonju 561-756, Korea
****Department of Veterinary Anatomy, College of Veterinary Medicine, Chonbuk National University, Duckjin-dong 1-Ga, Duckjin-gu, Jeonju 561-756, Korea
*****Division of Pharmaceutical Engineering, Woosuk University, Samnye-ro, Samnye-eup, Wanju 565-701, Korea
******HYOLIM E&I. Co., Ltd., 72, Achasan-ro 78-Gil, Gwangjin-gu, Seoul 143-802, Korea
(*Received 21 August 2013 • accepted 15 October 2013*)

Abstracts−The models of stenosed blood vessel with three different types of stenosis types have been modeled to investigate blood flow characteristics. The study was performed to investigate various hemodynamics, such as pressure and wall shear stress (WSS), with the change of stenosis ratio and Reynolds numbers (Re). The results of modeling, the minimum WSS occurred in different regions according to the stenosis types. The change of the diameter of blood vessel showed up in the pre-stenotic region by elastic behavior characteristics of blood vessels. Also, when the thickness of wall of blood vessel is 2 mm, the radius of blood vessel is increased by approximately two-times. As atherosclerosis progresses, the wall of blood vessels gradually loses elasticity and then the thickness of blood vessels gets thinner.

Keywords: Abdominal Aortic Aneurysm, Computational Fluid Dynamics (CFD), Atherosclerosis, Shear Stress

INTRODUCTION

Angina pectoris, which is ischemic heart disease, and myocardial infarction caused by atherosclerosis are becoming the main cause of death in the modern society and phenomena in which blood vessels are narrowing or clogging due to the atherosclerotic material (plaque). If the endothelial cells are injured along the wall of blood vessels, platelets are attached to it. If this injury continues, chunks of blood clot are accumulated. Thus, it becomes bigger and the blood vessel is clogged over time. Such atherosclerosis begins with dysfunction of endothelial cells. Changes in hemodynamic characteristics as well as biochemical factors are recognized as the important factors to cause such a failure [1-5].

Ku et al. claim that flow disturbances caused by blood vessels change the shear stress acting on endothelial cells and pressure distribution, and the changes in shear stress and pressure caused by the flow disturbances produce the arterial occlusion [6,7], Fry et al. claim that endothelial cells of blood vessels are damaged in the regions which have high shear stress in blood vessels, and the formation of blood clots is facilitated [8]. Thus, stenosis is formed. In addition, Caro, et al. claim that the time in which blood flow stays in region with low shear stress of blood flow appearing in the blood vessels is increased so that substances included in blood such as low-density lipoprotein (LDL) penetrate the wall of blood vessel and the atherosclerosis progresses [9]. When we adopt an approach to the occurrence of atherosclerosis in a specific region from a hemodynamic viewpoint, we can find the answer easily. The answer is that the hemodynamic characteristic becomes unstable. It is caused by the flow of blood which has the characteristics of turbulent flow or flow disturbance. The phenomenon of stenosis causes the pathological pains of heart attack and stroke.

An aneurysm is referred to as the abnormal expansion of the aorta. When it is increased by 1.5-fold over the normal diameter, it is conventionally determined to be an aneurysm [10,11]. If the diameter of the artery is increased, the pressure acting on the wall of aorta and the aorta is increased according to the law of Laplace. If the size of aneurysm is increased over time and reaches a certain limit, it cannot tolerate the pressure and it bursts. An important determining factor to predict the rupture of aneurysm is its size. Rupture occurs in more than 5 cm in the diameter of most aneurysms, but the rupture can occur in smaller size [12].

The size and distribution of shear stress in the wall of blood vessels is affected by blood flow determined by shape of the aneurysm. If blood flow is changed to a turbulent flow, additional stress caused by formation of turbulent flow acts on it. Because the shape of blood vessels varies in each person and information on flow is also varied, the shape of stenosis of blood vessels is shown differently and shape of the aneurysm is also shown differently based on the shape of ste-

†To whom correspondence should be addressed.
E-mail: kgb70@jbnu.ac.kr

nosis [13]. Changes in blood flow based on stenosis and subsequent shear stress, and the distribution of pressure and velocity become the important data on prediction of growth and rupture of aneurysm [14,15].

Currently, clinical professionals and scholars in the field of hemodynamics have made an effort to identify the causes of incidence of disease through clinical data on blood vessel diseases and hemodynamic characteristics. In vitro experiments for blood flow characteristics have many technical constraints, because of issues such as coagulation of blood, opacity and disposition problem of blood after experiment; the blood vessels have elastic behavior in the vertical direction to blood flow due to unsteady pulsatile flow produced by diastole and systole of the heart. The method to simulate the phenomenon of blood flow, which is difficult to test through a mathematical model and conduct the numerical analysis, has achieved many performances and it is being used [16,17].

The purpose of this study is to analyze the changes in the pressure inside blood vessels based on stenosis rate and shape in blood vessels and the distribution of load delivered into the blood vessels, and predict the effects on occurrence of aneurysm and rupture of blood vessels by using the computational fluid dynamics (CFD) method.

METHODS

A human abdominal aorta with combined stenosis and aneurysm was collected after surgical removing. Computational fluid dynamics model was constructed from 2D rational angiography images, a pulsatile flow calculation was performed and hemodynamic characteristics were analyzed. It was applied on the blood flow in abdominal aortic blood vessels in which stenosis occurred by using commercial finite element software ADINA Ver 8.5 (ADINA R & D, Inc., Lebanon, MA) fluid-solid interactions.

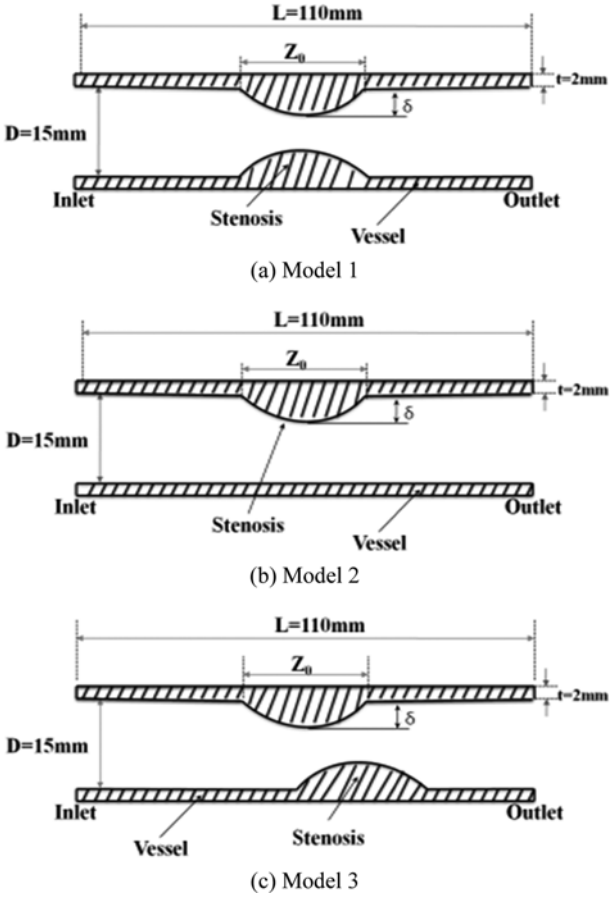

Fig. 1. Geometry of the stenosed blood vessel.

1. Numerical Model

The geometry of stenosed artery blood vessel shown in Fig. 1 was used in orer to analyze the blood flow of abdominal aortic blood vessels in which stenosis occurred. Model 1 was used to establish modeling for structure of symmetric stenosis. Model 2 was used to establish modeling for structure of stenosis occurring on one side. Model 3 was used to establish modeling for structure of nonsymmetric stenosis. The diameter (D) of abdominal aortic blood vessels was 15 mm and length (L) was 110 mm. The length (Z_0) of the part where stenosis occurred was 15 mm and the thickness of the vessel wall was 2 mm. Because the shape of stenosis was quite varied, there was no stylized shape. Therefore, geometric shape of the stenosed section in the numerical model was assumed as a cosine function and Eq. (1) was used. The variable (s) to represent the size of stenosed section was defined as Eq. (2) for stenosis ratio [18]. The stenosis ratios of 30, 50 and 70% were set depending on the extent of decrease of cross sectional area of blood vessel in the stenosed section in the numerical model [15].

$$\frac{r(z)}{R}=\begin{cases}1-\frac{\delta}{2}\left[1+\cos\left(\frac{\pi z}{z_0}\right)\right] & \text{if } |z|\le z_0\\ 1 & \text{if } |z|\ge z_0\end{cases} \quad (1)$$

$$s=(d-\delta)/d\times 100\% \quad (2)$$

2. Boundary Condition

It was assumed that the blood vessel wall was an elastic wall with a constant thickness. The density of the vessel wall was 2,000 [kg/m^3], Young's modulus was 0.7×10^6 [N/m], and Poisson ratio was 0.49. Blood used in this study was assumed as a uniform, incompressible and isothermal Newtonian-fluid and the density was 1,060 [kg/m^3] and viscosity was 0.0035 [kg/m·s], respectively [15]. Blood behaves as a non-Newtonian fluid at shear rates above 100 s^{-1} [19, 20], which may account for the Newtonian approximation in flow simulations at larger Reynolds numbers. The paper describes the calculation of an effective Newtonian viscosity which captures the non-Newtonian effects for this flow situation. Sud and Sekhon [21] presented a mathematical model for flow in single arteries subject to pulsatile pressure gradient as well as the body acceleration. In their analytical treatment, blood is assumed to be Newtonian fluid and flow as laminar, onedimensional, and tube wall as rigid and uniformly circular [22]. Fully developed flow was given as an inlet condition to analyze the characteristic of blood flow within the blood vessels in which stenosis occurred and numerical analysis with the velocity distribution of the Reynolds number (Re) of 500, 800 and 1,200 at the inlet was carried out. In addition, continuous flow and pulsatile flow, which had the regular shape in the form of a sine function, were given as an inlet condition. If the flow is pulsatile as an inlet condition, it was assumed that the velocity distribution changed with the sine wave form without the occurrence of the reflux of 1 Hz.

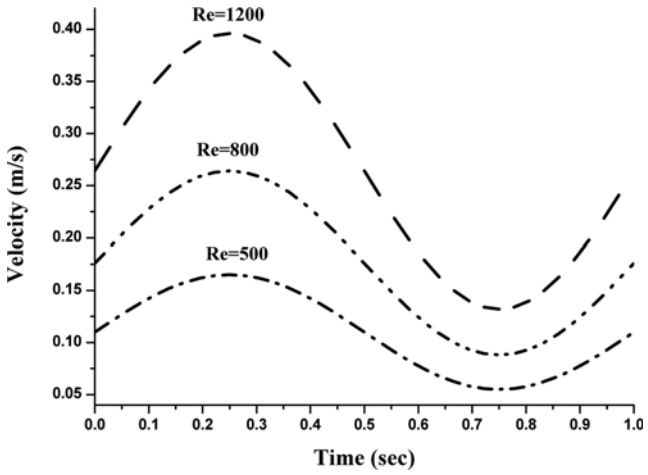

Fig. 2. The pulsatile velocity profile at the inlet with the change of Reynolds numbers.

The initial velocity based on Re was calculated using Eq. (3) [15].

$$U(t)=\overline{U}(1+0.5\sin 2\pi t) \quad (3)$$

Fig. 2 shows the velocity distribution depending on time used in the inlet condition at the pulsatile flow. The velocity based on time had the maximal value at t=0.25 s and the minimal value at t=0.75 s.

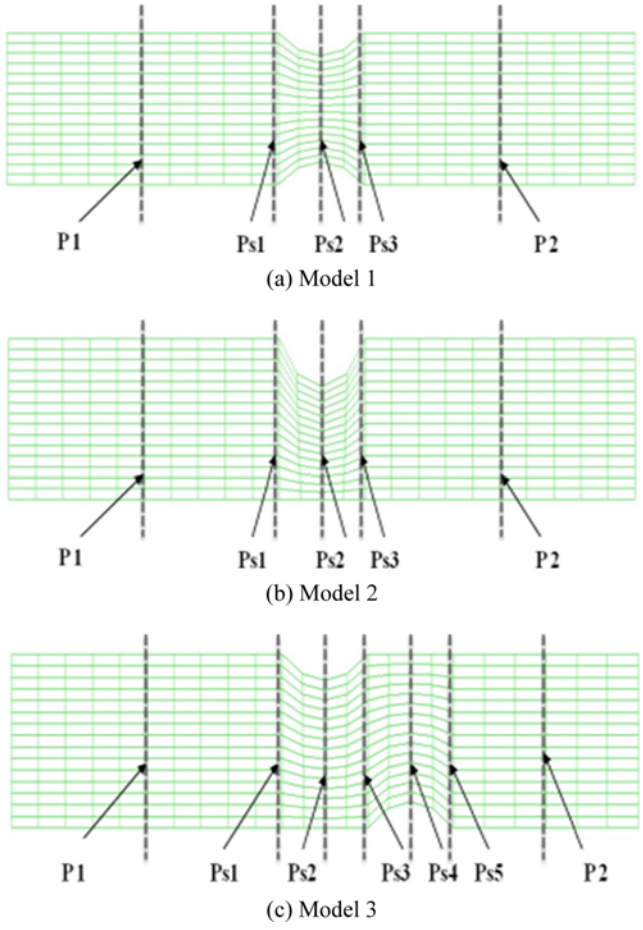

Fig. 3. Grid mesh used in the fluid and solid models.

In case of the pulsatile flow, the blood vessel wall was assumed as an elastic wall, and systole and diastole are repeated depending on the fluid flow. No-slip condition was used in blood vessel wall.

In this study, the iteration method was set to repeat it up to 15 times per a step by using the Newton method, and then it was calculated. A direct computing method with good convergence was used as the method to interpret the fluid-structure interaction (FSI) model. FCBI (flow condition based interpolation) element was used for fluid element formulation.

Fig. 3 shows the grid generation model based on structure in which stenosis occurs. In Models 1 and 2, P1 represents the center point of the region before stenosis. Ps1 represents the start point of stenosis. Ps2 represents the center point of stenosis. Ps3 represents the end point of stenosis. P2 represents the center point of the area after stenosis. In model 3, P1 represents the center point of the area before stenosis. Ps1 represents the start point of the first stenosis. Ps2 represents the center point of the first stenosis. Ps3 represents the end point of the first stenosis. Ps4 represents the center point of the second stenosis. Ps5 represents the end point of the second stenosis. In case of total elements of generated grid, there are 96 structural models and 360 fluid models.

RESULTS AND DISCUSSION

Fig. 4 shows the pressure distribution based on changes in the stenosis rate. Fig. 4(A) shows the pressure distribution in continuous flow. Average pressure is increased linearly from the entrance region to Ps1, but it is rapidly decreased after Ps1. A minimum value is shown in Ps2, but the pressure is not changed after Ps3. In model 1, when the stenosis rate is 70% and Reynolds number is 1200, the maximum velocity is approximately 13 times as high as that when the stenosis rate is 30%. It is approximately 5.5 times as high as that in model 2. It is approximately 4.5 times as high as that in model 3. In case of model 1 with symmetric stenosis, as the stenosis rate is increased, the maximum pressure is shown in the region ahead of Ps1. As the Reynolds number and stenosis rate is increased, a significant change in pressure is shown. Fig. 4(B) show the average pressure based on changes in the stenosis rate during diastole and systole in pulsatile flow. When the stenosis rate is 30% during diastole, the average pressure is the lowest in the entrance region and it is the highest in the exit region. In case of low stenosis rate, the average pressure generally has a negative value. High pressure is shown in the region ahead of Ps1 with increasing stenosis rate and Reynolds number. When the stenosis rate is more than 50%, the lowest pressure is shown at Ps2 in models 1 and 2, and it is shown at Ps4 in model 3. When the stenosis rate is more than 70%, the pressure drop gets bigger with increasing Reynolds number. The average pressure during systole is similar to the result of a continuous flow and its value is relatively high. The pressure in the blood vessel gradually increases until it reaches the Ps1, and it is rapidly decreased at Ps1. The lowest value is shown at Ps2 in models 1 and 2, and at Ps4 in model 3. The maximum pressure is shown at P1 in models 1 and 2, and at Ps1 in model 3. In the case of low stenosis rate, the pressure tends to be increasing after Ps3 and then decreasing. We suggest that pressure distribution across the stenosis is more important for atherosclerotic material (plaque) vulnerability. There is a pressure drop across the atherosclerotic material because of the

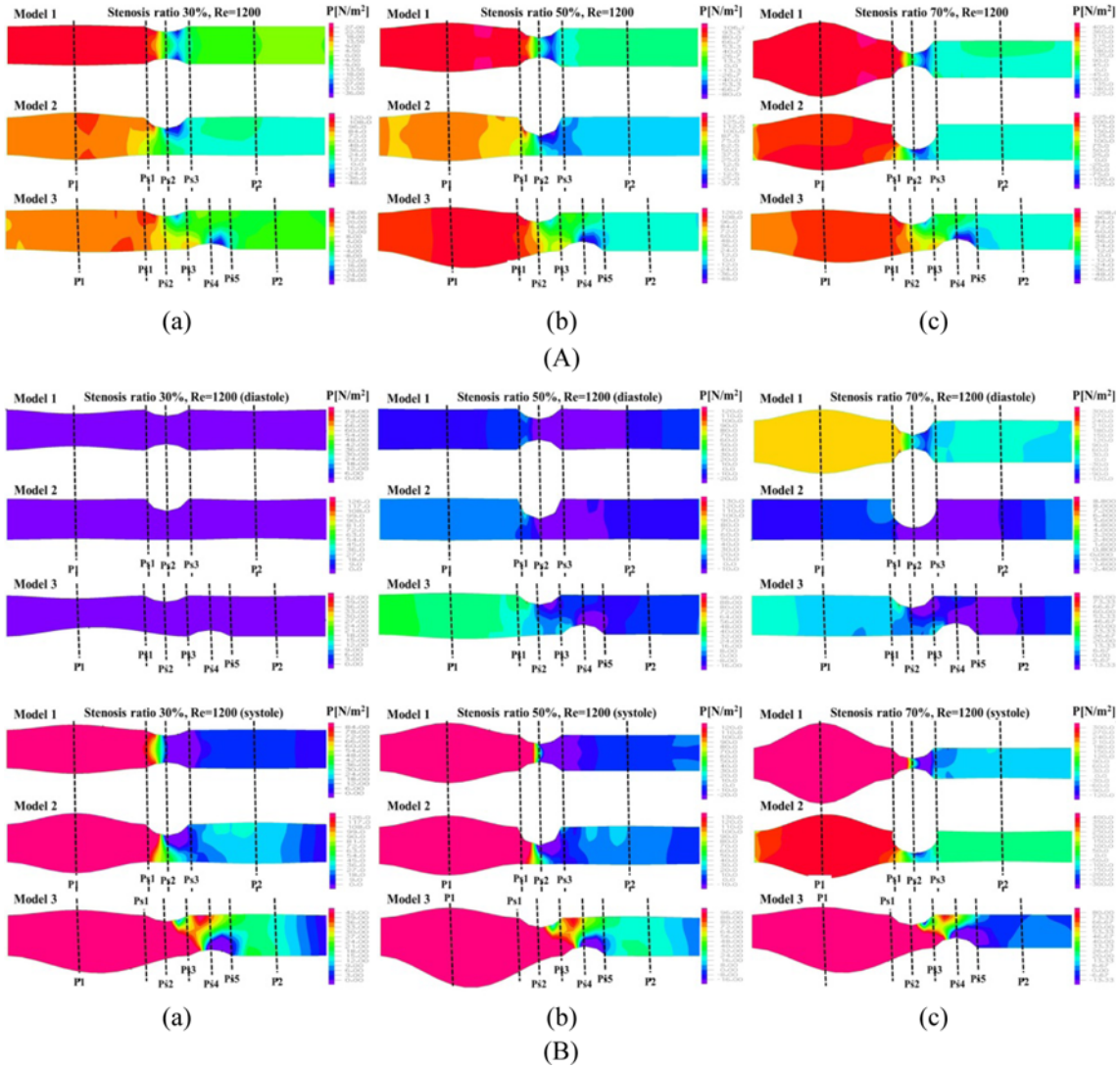

Fig. 4. The pressure distribution with stenosis ratio in the continuous flow (A) and pulsatile flow (B). (a) Stenosis ratio 30%, (b) Stenosis ratio 50%, (c) Stenosis ratio 70%.

stenosis. According to the Bernoulli principle, this increased blood velocity produces a lower lateral blood pressure acting on the atherosclerotic material. Thus, a pressure gradient build-up is created across the atherosclerotic material that could rupture it. Any increase in systemic pressure or increase in the narrowing of the lumen would further increase the velocity through the narrowed lumen and increase the pressure drop [23,24].

Fig. 5 shows wall shear stress (WSS) acting on the wall of blood vessel based on changes in the stenosis rate. Fig. 5(A) shows WSS in continuous flow. WSS implies the hemodynamic force acting on the inner wall of blood vessel due to the flow field in blood vessel. Such WSS is closely associated with growth of stenosis part in a blood vessel and rupture of the blood vessel. In addition, it has been known that intimal thickening occurs easily in area with low wall shear stress. Such intimal thickening progresses as the initial atherosclerotic plague [25]. WSS is rapidly decreased at Ps1 and it is gradually increased at Ps3. Rapidly reduced WSS is shown at Ps2 and maximum WSS is shown at P1. Model 2 shows the biggest change in shear stress and model 3 shows the smallest change in shear stress. In addition, as stenosis and Reynolds number are increased, maximum WSS is increased and minimum WSS is decreased. Therefore, it is thought to be highly likely to be exposed to the atherosclerosis with increasing stenosis rate. Fig. 5(B) shows the WSS acting on wall of blood vessel during diastole and systole in pulsatile flow. When the stenosis rate is 30% during diastole, the minimum shear stress is shown at P1 in models 1 and 3, and it is shown at Ps2 in model 2. In addition, the minimum shear stress is moving toward the entrance region with increasing Reynolds number in model 3. When the stenosis rate is more than 50%, the minimum shear stress is moving toward the entrance region with increasing Reynolds number in models 1 and 2. When the stenosis rate is 70%, the shear stress is significantly changed in the region after Ps2 with increasing Reynolds number. The WSS acting on the wall of blood vessel during systole shows the highest changes in shear stress in model 1 and the lowest changes in shear stress in model 3. Changes in shear stress are getting bigger with increasing Reynolds number. High shear stress is shown in the region ahead of Ps1 and it has a negative value in the region after Ps1. The maxi-

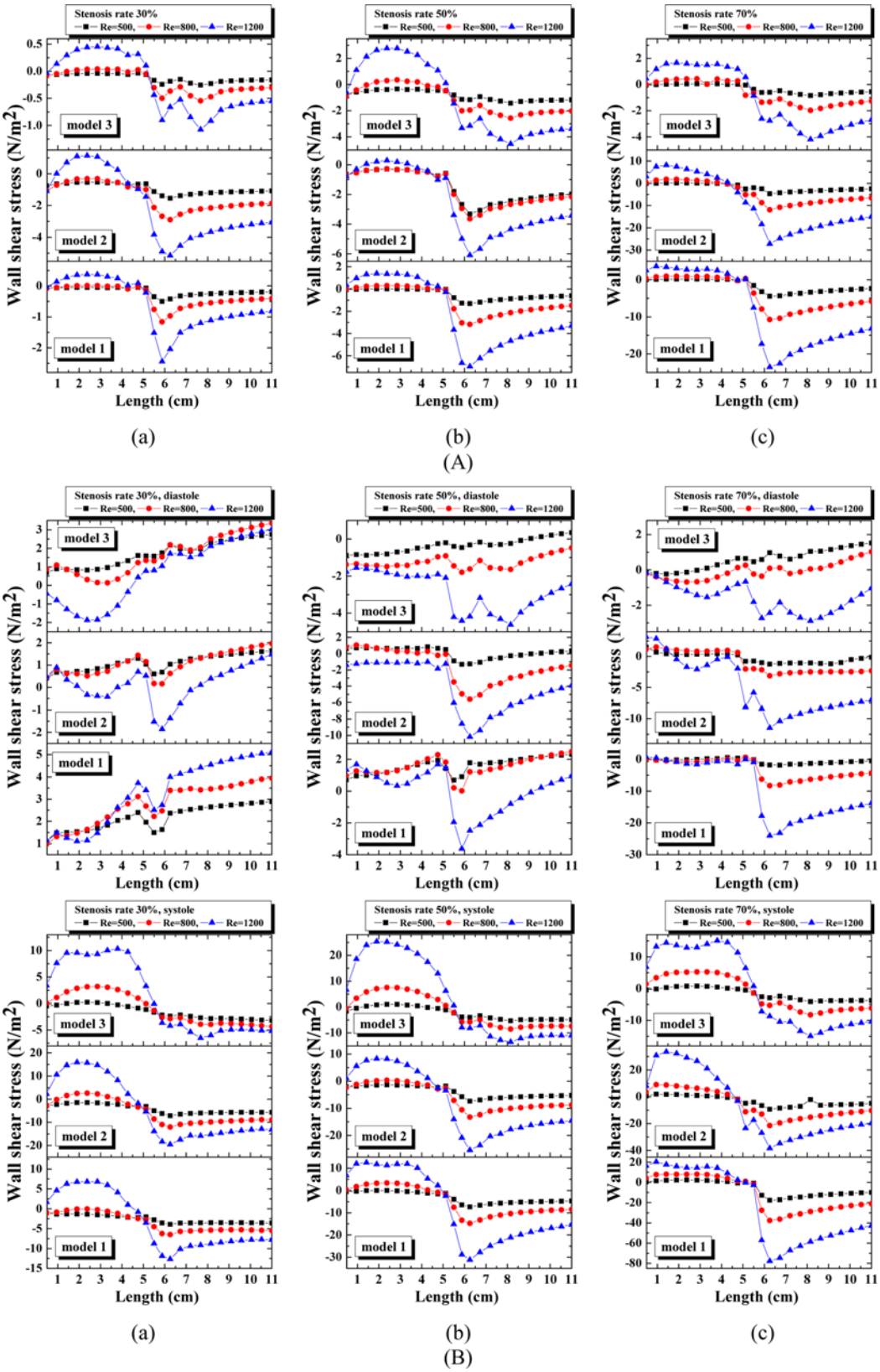

Fig. 5. The shear stress with stenosis ratio in the continuous flow (A) and pulsatile flow (B). (a) Stenosis ratio 30%, (b) Stenosis ratio 50%, (c) Stenosis ratio 70%.

mum shear stress is increased with increasing stenosis rate and Reynolds number and the minimum shear stress is decreased. P1 in which maximum shear stress is formed is predicted to be the region where structure of wall of blood vessel is likely to be changed. This region

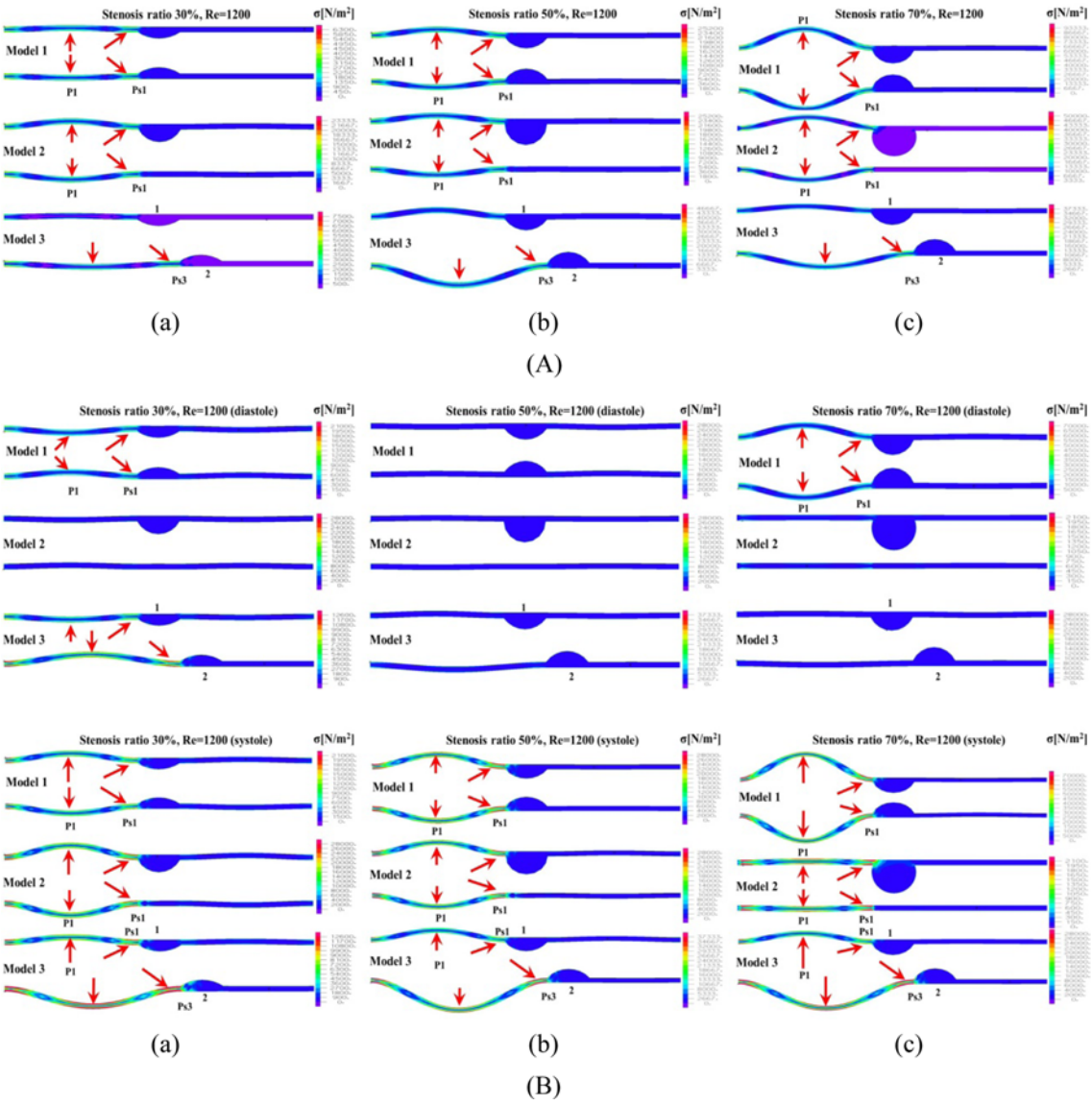

Fig. 6. The wall shear stress distribution with stenosis ratio in the continuous flow (A) and pulsatile flow (B). (a) Stenosis ratio 30%, (b) Stenosis ratio 50%, (c) Stenosis ratio 70%.

is thought to be the stagnation point of blood in which platelets, which are a blood parameter, begin to be deposited in the internal wall of the blood vessel and cause blood clots to form. Platelets which receive high shear stress are stagnant at P1 due to the recirculation vortex, and more likely to be attached on wall of blood vessels with increasing time. In these regions, blood clots are prone to occur and aneurysms are frequently formed in regions where blood clots are formed on internal walls of blood vessels [26,27]. In all models, points where the maximum shear stress is formed are almost same, but the points where the minimum shear stress is formed are shown differently. Asymmetry of stenosis shape is found to have a big impact on changes in shear stress. Atherosclerotic material stress may be a more important factor when the mechanism of atherosclerotic material rupture is considered [28-32]. The arterial wall continuously interacts with hemodynamic forces, which include WSS and blood pressure. Atherosclerotic material stress is the result of external hemodynamic forces. Atherosclerotic material rupture itself represents structural failure of a component of the diseased vessel, and it is therefore reasonable to propose that the biomechanical properties of atheromatous lesions may influence their vulnerability to rupture [23,24].

Fig. 6 shows the distribution of load acting on the wall of blood vessels based on changes in the stenosis rate. Fig. 6(A) represents continuous flow. Fig. 6(B) represent the distribution of load acting on wall of blood vessels in pulsatile flow. In models 1 and 2, P1 and Ps1 get more loads. It is thought that the flow of blood at P1 is not smooth due to stenosis of blood vessels and the diameter of a blood vessel is increased and the load of the blood vessels was is increased by movement load of blood acting on blood vessels. In addition, since the diameter of blood vessels is increased at P1, many loads and flow energy of blood are concentrated at Ps1. Thus, it is expected that load blood vessels wall at Ps1 is shown high. In model 3, however, many loads are applied in the region between P1 and Ps1, and many loads are concentrated at Ps3. In addition, as shown

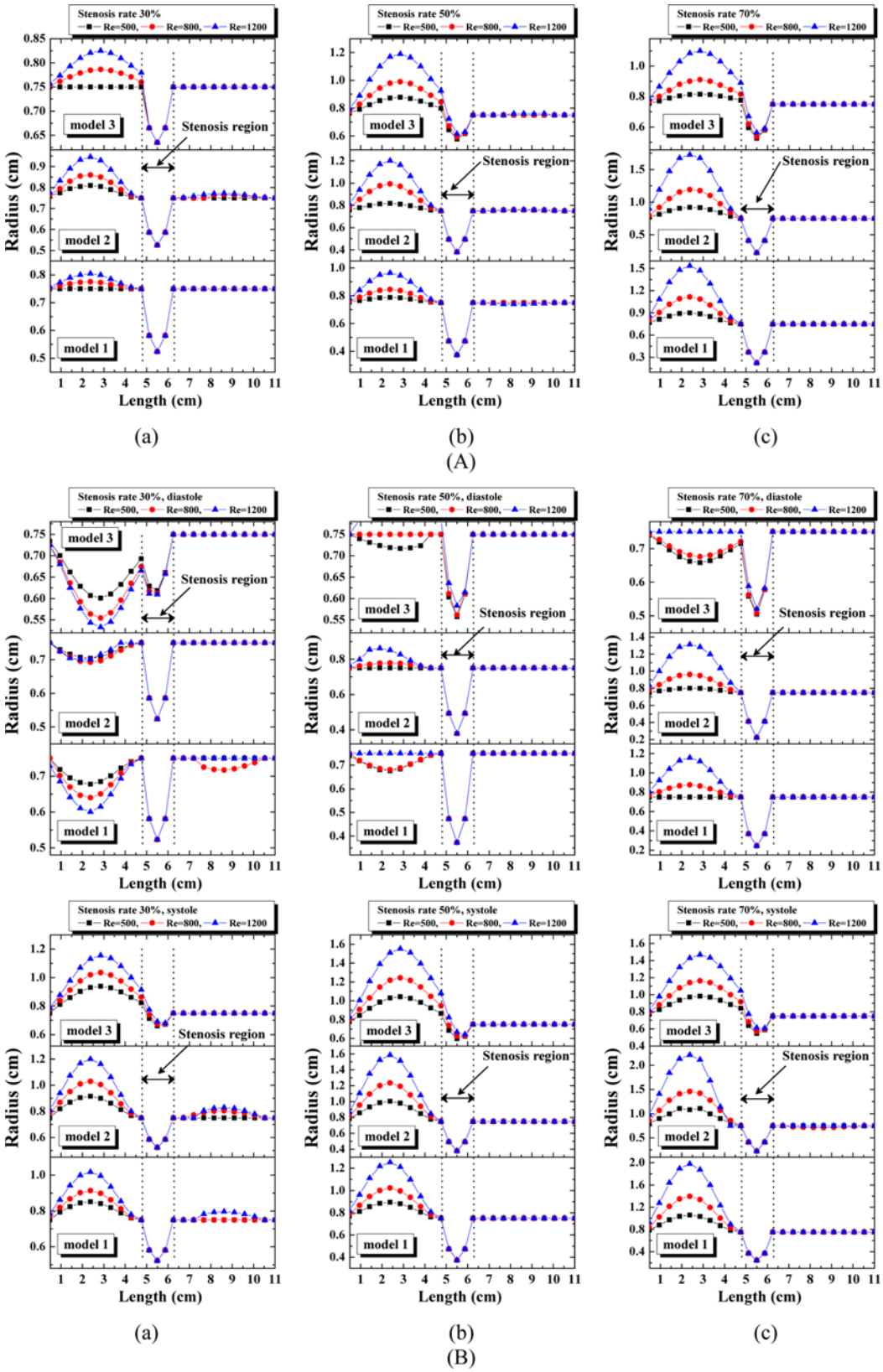

Fig. 7. The radius change of blood vessel with stenosis ratio in the continuous flow (A) and pulsatile flow (B). (a) Stenosis ratio 30%, (b) Stenosis ratio 50%, (c) Stenosis ratio 70%.

in results of a continuous flow, many loads are concentrated at P1 and Ps1 during diastole. However, many loads are concentrated at P1, Ps1, Ps3 and the region between P1 and Ps1 during systole. When the results of modeling are reviewed, the load acting at P1 and the

region between P1 and Ps1 increases the diameter of blood vessels, but it is expected that it may not have a significant impact on destruction of blood vessels, if it is not operated over the limits of elasticity of blood vessels. Because loads concentrated at Ps1 and Ps3 are relatively higher than those in other regions, if the destruction of blood vessels occurs, this place is expected to occur. However, because the results of this study are made by modeling, it is thought that it may be different from actual clinical cases.

Fig. 7 shows the changes in the radius of blood vessel based on changes in the stenosis rate. Fig. 7(A) shows the change in the radius of blood vessel in continuous flow. Radius displacement of blood vessel is made due to elastic behavior of blood vessel as blood flow is changed. Due to unstable blood flow in blood vessels where stenosis occurs, the phenomena occur in which pressure is increased and blood vessel is swollen in the region ahead of stenosis. Such expansion of blood vessels may cause an abdominal aortic aneurysm. The criterion to determine abdominal aortic aneurysm is the increase of the blood vessel diameter, which is 1.5 times as high as normal diameter. The diameter of blood vessels is increased by more than 1.5 times in all models when the stenosis rate is 50% and Reynolds number is 1200, and in models 1 and 2 when the stenosis rate is 70% and Reynolds number is more than 800. In addition, in model 3, the diameter of blood vessels is increased by more than 1.5 times when the Reynolds number is more than 1200. Thus, it is thought that an aneurysm occurs. When the stenosis rate is the same, the biggest change in radius is shown in model 2 and the smallest change is shown in model 3. In addition, the bigger changes in radius are shown with increasing stenosis rate and Reynolds number. Unlike changes in the radius of blood vessel in region ahead of stenosis, there are almost no changes in the radius of blood vessel in regions after stenosis. Therefore, it is thought that shape of stenosis does not affect the changes in the radius of region after stenosis. Fig. 7(B) show the change in the radius of blood vessel in pulsatile flow. When the stenosis rate is low during diastole, the radius of the blood vessel tends to be decreased in the region ahead of Ps1. However, the vasoconstriction caused by such reduction of the radius of blood vessel is restored again by the elastic behavior of blood vessels during systole. However, the radius of blood vessels is increased and the phenomenon of swelling blood vessels is shown in the region ahead of Ps1 with increasing stenosis rate and Reynolds number. Due to the nature of unstable blood flow with increasing stenosis rate, excessive contraction and relaxation of blood vessels are repeated and then blood vessels lose the elastic property and high pressure is given in this region. During diastole, the changes in the radius are the biggest in model 2 and the smallest in model 3. However, changes in the radius are almost not shown in the region after stenosis. When the stenosis rate is 30% during systole, the radius of blood vessel tends to be increased in the region after Ps3 due to the elastic property of blood vessel as accelerated blood flow goes through Ps2 in region of stenosis in models 1 and 2. When the stenosis rate is 50% in models 1 and 3, similar changes in the radius are shown. It is the highest in model 2. When the stenosis rate is 70% in models 1 and 2, similar changes in the radius are shown. It is the lowest in model 3.

Fig. 8 is the result of previous study showing changes in the radius of blood vessels based on changes in the stenosis rate when the thickness of wall of blood vessel is 1 mm [14,15]. In the result of previous study, the shape of stenosis part is the same as that in the model 1.

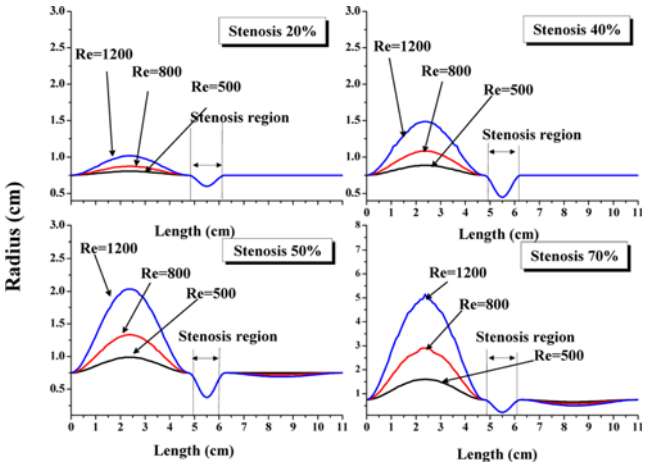

Fig. 8. A radius change of blood vessel (Blood vessel wall thickness 1 mm).

When the stenosis rate is 70% and Reynolds number is 1200 in thickness of wall of blood vessel of 1 mm, the radius of blood vessels is increased by approximately 6.8 times. When the wall thickness of blood vessels is 2 mm, the radius of blood vessels is increased by approximately 2 times. When compared with results of previous studies, thickness of the wall of blood vessels affects the changes in the radius of blood vessels.

Table 1 shows the maximum extended diameter of blood vessels at pre-stenosed section. Table 1 shows the results when the thickness of wall of blood vessel is 2 mm (a) and 1 mm (b), respectively. According to clinical statistical data, when the diameter of blood vessels is more than 4 cm, the aneurysm ruptures. When the diameter of blood vessels is 4-5 cm, the risk of rupture is about 0.5-5%. Fluid velocity, atherosclerotic material deformation, and atherosclerotic material internal stress were calculated. A stress of 300 KPa was used as the threshold to indicate high risk of atherosclerotic material rupture. After data analysis, Li et al concluded that there is a direct correlation between the degree of stenosis and the thickness of the fibrous cap [31]. It is common practice for physicians to perform surgery for stenosis greater than 70% due to high rupture risks [33.34]. Li et al., show in the results that there is still a high risk for rupture of stenosis between 30% and 70% depending on the thickness of the fibrous cap. The critical thickness for this range of stenosis was showed to be 0.5 mm [31]. However, when the diameter of blood vessels is more than 7 cm, the risk of rupture is increased up to 20-40%. From the result of experiments with thickness of blood vessels of 1 mm, when the stenosis rate is more than 50%, the risk of rupture of aneurysm is shown. From experiments with thickness of blood vessels of 2 mm, the risk of rupture of aneurysm is not shown. As the stenosis progresses, the diameter of blood vessels is increased in all areas of stenosis. The diameter of blood vessels is significantly increased as the thickness of wall of blood vessels gets thinner. Increase in such stenosis rate and diameter of blood vessels in all regions of stenosis is thought to increase the risk of rupture of blood vessels together with occurrence of aneurysm. The relationship between diameter and rupture of blood vessels of abdominal aortic aneurysm is being reported through clinical cases each year, and a high mortality rate is produced in the abdominal aortic aneurysm. In addition, as atherosclerosis progresses, the walls

Table 1. Maximum extended diameter of pre-stenosed section with stenosis ratio. (a) blood vessel wall thickness=2 mm, (b) blood vessel wall thickness=1 mm

(a)

S (%) / Re	30			50			70		
	Model 1	Model 2	Model 3	Model 1	Model 2	Model 3	Model 1	Model 2	Model 3
500	1.5 No grown	1.62 Grown 1.08 times	1.5 No grown	1.58 Grown 1.05 times	1.64 Grown 1.09 times	1.75 Grown 1.17 times	1.8 Grown 1.2 times	1.84 Grown 1.23 times	1.63 Grown 1.09 times
800	1.55 Grown 1.03 times	1.72 Grown 1.15 times	1.57 Grown 1.05 times	1.69 Grown 1.13 times	1.99 Grown 1.33 times	1.98 Grown 1.32 times	2.23 Grown 1.49 times	2.38 Grown 1.59 times	1.82 Grown 1.21 times
1200	1.61 Grown 1.07 times	1.9 Grown 1.27 times	1.65 Grown 1.1 times	1.93 Grown 1.29 times	2.41 Grown 1.61 times	2.38 Grown 1.59 times	3.07 Grown 2.05 times	3.45 Grown 2.3 times	2.2 Grown 1.47 times

(b)

S (%) / Re	20	40	50	70
500	1.61 Grown 1.07 times	1.77 Grown 1.18 times	1.97 Grown 1.31 times	3.21 Grown 2.14 times
800	1.75 Grown 1.16 times	2.16 Grown 1.44 times	2.67 Grown 1.78 times	5.81 Grown 3.87 times
1200	2.03 Grown 1.35 times	2.97 Grown 1.98 times	4.07 Grown 2.71 times	10.3 Grown 6.87 times

of blood vessels gradually lose elasticity and then blood vessels get thinner. Therefore, the change in the diameter of the blood vessels is helpful to understand the relationship between occurrences of atherosclerosis and aneurysm, and it is an important determining factor to predict the rupture of aneurysm.

CONCLUSIONS

Blood flow in blood vessels in which stenosis occurs shows many differences compared with that in a healthy condition. In addition, hemodynamic characteristics are various based on the morphological characteristics of blood vessels, and the possibility and progress of aneurysm may vary. If stenosis forms in blood vessels, smooth flow is disturbed and the pressure drop increases. The pressure drop is increased and the changes in velocity are also shown significantly with increasing stenosis rate and the Reynolds number. When the stenosis rate is the same, the pressure drop in velocity is bigger in symmetric structure than that in asymmetric structure. Changes in the WSS show the maximum value in all regions of stenosis and the minimum value is shown in the part of stenosis. The minimum shear stress is formed in different locations based on the stenosis shape model. It is thought that the regions with high shear stress may destroy or damage blood endothelial cells, and the regions with low shear stress may damage the blood vessels by increasing stagnation time of blood flow. The maximum WSS is increased and the minimum WSS is decreased with increasing stenosis rate and Reynolds number. Because the occurrence of stenosis in blood vessels may affect the elastic behavior of blood vessel walls, it is expected that the pressure is increased due to unstable blood flow and an aneurysm, which is the phenomenon of swelling blood vessel, occurs in all regions of stenosis. The radius of blood vessels is increased in all regions of stenosis with increasing stenosis rate, and it is expected that the stenosis shape has a big impact on changes in the radius of blood vessels.Through such studies, it is thought that characteristics of blood flow in the abdominal aorta where stenosis is formed will be helpful to understand the mechanism of growth of atherosclerosis, and the occurrence and rupture of abdominal aortic flow.

ACKNOWLEDGEMENTS

This work was supported by National Research Foundation of Korea Grant funded by the Korean Government (Ministry of Education, Science and Technology (NRF-2010-359-D00036) and the fund of Chonbuk National University Hospital Research Institute of Clinical Medicine.

REFERENCES

1. D. P. Giddens, C. K. Zarins and S. Glagov, *J. Biomech. Eng. T. ASME*, **115**, 588 (1993).
2. B. K. Lee, H. M. Kwon, D. S. Kim, Y. W. Yoon, J. K. Seo, I. J. Kim, H. W. Roh, S. H. Suh, S. S. Yoo and H. S. Kim, *Yonsei Med. J.*, **39**(2), 166 (1998).
3. G. R. Zendehbudi and M. S. Moayeri, *J. Biomech.*, **32**, 959 (1999).
4. B. K. Lee, H. M. Kwon, B. K. Hong, B. E. Park, S. H. Sug, M. T. Cho, C. S. Lee, M. C. Kim, C. J. Kim, S. S. Yoo amd H. S. Kim, *Yonsei Med. J.*, **42**(4), 375 (2001).
5. H. K. Kim, J. C. Park, S. S. Kim, H. S. Choi, D. S. Sim, N. S. Yoon, H. J. Yoon, Y. J. Hong, H. Y. Park, J. H. Kim and Y. G. Yan, *Korean J. Int. Med.*, **77**, 68 (2009).

6. D. N. Ku, D. P. Giddens, C. K. Zarins and S. Glagov, *Arteriosclerosis*, **5**, 293 (1985).
7. D. Bluestein, Y. Alemu, I. Avrahami, M. Gharib, K. Dumont, J. J. Ricotta and S. Einav, *J. Biomech.*, **41**, 1111 (2008).
8. D. L. Fry, *A Ciba Foundation Symp*., ASP, Amsterdam, The Netherlands, 40 (1972).
9. C. G. Caro, F. M. Fitz-Gerald and R. C. Schroter *Proc. R. Soc. B*., **177**, 109 (1971).
10. R. W. Thompson, P. J. Geraghty and J. K. Lee, *Curr. Prob. Surg.*, **39**(2), 110 (2002).
11. M. F. Fillinger, S. P. Marra, M. L. Raghavan and F. E. Kennedy, *J. Vasc. Surg.*, **37**(4), 724 (2003).
12. S. E. Oh and K. R. Lee, *J. Biomed. Eng. Res.*, **21**(2), 181 (2000).
13. A. Valencia and M. Villanueva, *Int. Commun. Heat Mass Transf.*, **33**, 966 (2006).
14. S. J. Kim, Y. R. Park, S. J. Kim, H. S. Kang, J. S. Kim, S. H. Oh, S. J. Kang and G. B. Kim, *JKAIS*, **13**(5), 2285 (2012).
15. Y. R. Park, S. J. Kim, S. J. Kim, J. S. Kim, H. S. Kang and G. B. Kim, *J. Biomed. Nanotechnol.*, **9**, 1137 (2013).
16. J. H. Choi, C. S. Lee and C. J. Kim, *J. Biomed. Eng. Res.*, **21**(4), 363 (1997).
17. S. H. Seo, J. K. Park, H. W. Roh, B. K. Lee and H. M. Kwon, *Trans. KSME, B*, **34**(10), 893 (2010).
18. N. K. David, *Ann. Rev. Fluid Mech.*, **29**, 399 (1997).
19. A. Kirpalani, H. Park, J. Butany and K. W. Johnston, *J. Biomech. Eng.*, **121**(4), 370 (1999).
20. R. Manimaran, *WASET*, **49**, 957 (2011).
21. V. K. Sud and G. S. Sekhon, *Bull. Math. Biol.*, **47**, 35 (1985).
22. K. C. Ro and H. S. Ryou, *Korea-Aust. Rheol. J.*, **21**(3), 175 (2009).
23. Z. Y. Li and J. H. Gillard, *J. Am. Coll. Cardiol.*, **52**(6), 498 (2008).
24. Z. Y. Li, V. Taviani, T. Tang, U. Sadat, V. Young, A. Patterson, M. Graves and J. H. Gillrd, *BJR*, **82**, S39 (2009).
25. D. M. Wootton and D. N. Ku, *Annu. Rev. Biomed. Eng.*, **1**, 299 (1999).
26. M Ojha, *J. Biomech.*, **26**, 1379 (1993).
27. M. Mittal, S. P. Simmons and H. S. Udaykumar, *J. Biomech. Eng. T. ASME*, **123**, 325 (2001).
28. G. C. Cheng, H. M. Loree, R. D. Kamm, M. C. Fishbein and R. T. Lee, *Circulation*, **87**, 1179 (1993).
29. R. T. Lee, H. M. Loree, G. C. Cheng, E. H. Lieberman, N. Jaramillo and F. J. Schoen, *J. Am. Coll. Cardiol.*, **21**, 777 (1993).
30. Z. Y. Li, S. Howarth, R. A. Trivedi, J. M. UK-I, M. J. Graves, A. Brown, L. Wang and J. H. Gillard, *J. Biomech.*, **39**, 2611 (2006).
31. Z. Y. Li, S. P. Howarth, T. Tang and J. H. Gillard, *Stroke*, **37**, 1195 (2006).
32. Z. Y. Li, S. P. Howarth, T. Tang, M. J. Graves, J. M. UK-I, R. A. Trivedi, P. J. Kirkpatrick and J. H. Gillard, *J. Vasc. Surg.*, **45**, 768 (2007).
33. MRC European Carotid Surgery, *Lancet*, **337**, 1235 (1991).
34. North Americas Symptomatic Carotid Endarterectomy Trial collaborators, *N. Eng. J. Med.*, **325**, 445 (1991).